Renewable and Sustainable Energy Reviews 19 (2013) 11–17

Contents lists available at SciVerse ScienceDirect

Renewable and Sustainable Energy Reviews

journal homepage: www.elsevier.com/locate/rser

Maximum power point matching versus maximum power point tracking for solar generators

Alon Kuperman [a,*], Moshe Averbukh [b], Simon Lineykin [c]

[a] Department of Electrical Engineering and Electronics, Ariel University Center of Samaria 40700, Israel
[b] Department of Solar Energy & Environmental Physics, Ben-Gurion University of the Negev, 84990, Israel
[c] Department of Mechanical Engineering and Mechatronics, Ariel University Center of Samaria, 40700, Israel

ARTICLE INFO

Article history:
Received 2 October 2012
Accepted 5 November 2012
Available online 30 November 2012

Keywords:
Solar Array
Load matching
MPPT

ABSTRACT

In this paper, a method of designing an optimally arranged solar array for converterless matching to a known linear load is proposed and compared to the classical Maximum Power Point Tracking method. Long-time performance of both methods is examined for three common types of loads under real weather conditions. Test results indicate that only in case of a pure resistive load the Maximum Power Point Tracking-based solar system advantage is undisputed. In case of a load represented by a voltage source with internal resistance, the long term energy productions of the system employing a practical Maximum Power Point Tracking operated converter is on a par or lower than the converterless system energy yield.

Contents

1. Introduction

Photovoltaic (PV) power is probably the strongest-growing electricity generating technology, demonstrating recent annual growth rates of around 40% and world production of 10.66 GW in 2009, consisting of both off-grid remote power supplies and residential-roof grid-connected systems [1]. Large increases in global cumulative PV capacity are foreseen for the next decade in case economic incentives are supported long enough. Besides playing a significant role in the future energy fusion, PV generation is significantly contributing to the environmental impact of electricity supply [2].

PV technology is one of the best ways to harvest the solar energy, since PV devices are strong and simple in design, requiring very little maintenance and capable of giving outputs from microwatts to megawatts. This is why they are used as power sources in water pumping, remote buildings, solar home systems, communications, satellites and space vehicles, reverse osmosis plants, and even megawatt-scale power plants [3]. The efficiency still remains the main weakness of the technology. When exposed to unconcentrated sunlight, modern solar cells are struggling to reach the theoretical thermodynamic efficiency limits (40.6% and 63.6% for single and triple junction cells, respectively). Hence, further electrical conversion losses must be minimized in order to increase the feasibility of PV-based energy production in addition to maximizing the amount of solar energy captured by the collector [4]. The problem of developing tracking schemes capable of following the trajectory of the sun throughout the course of the day on a year-round basis has received significant coverage in the literature [5]. Although using sun tracker is not essential, it can significantly boost the collected energy in different periods of time and geographical conditions in large solar fields [6].

Nevertheless, the importance of both cell efficiency and amount of solar energy captured by the collector is marginal if

* Corresponding author. Tel.: +972 5269 43234.
E-mail address: alonku@ariel.ac.il (A. Kuperman).

1364-0321/$ - see front matter © 2012 Elsevier Ltd. All rights reserved.
http://dx.doi.org/10.1016/j.rser.2012.11.012

the solar array (SA) is incorrectly matched to the load. The output of the most efficient cell under very rich illumination can still yield low power output if the electrical operating point is improper. As a matter of fact, the electrical characteristic curve of a solar cell possesses a single maximum power point (MPP) for a given temperature and solar irradiance. Hence, correct SA sizing and matching to the load in order to extract maximum possible power is of an extreme significance [7–11].

There are two main classical approaches to SA–load matching: a passive approach, referred hereafter as maximum power point matching (MPPM); and an active approach, referred henceforth as maximum power point tracking (MPPT). The passive approach principle is based on designing a SA suited to the load such that while operating under nominal conditions, the operating point coincides with the SA MPP. The main drawbacks of the approach are the necessity of the voltage level matching between the SA and the load and the fact that the MPP moves away from the operating point when the environmental conditions are no longer nominal. The main advantage of the method is a glueless SA–load connection, allowing reducing the cost, weight, volume and losses as a result of intermediate conversion stage absence [12–17].

The active matching method is based on inserting a power converter between the SA and the load in order to force the SA operating point follow the MPP upon the environmental conditions variation. The MPPT approach eliminates the SA–load voltage matching requirement and allows instantaneous MPP operation at the expense of additional hardware and control effort (and hence increased cost, volume and weight). Moreover, additional losses caused by an additional conversion stage presence must be taken into account. MPPT algorithms have evolved over the last two decades along with the tremendous increase of the computational power and power semiconductor technology progress. A great variety of MPPT approaches were proposed in the literature and summarized in several review papers [18–23], while different topologies of the MPPT-operated power converters were evaluated in [24–30]. It should be mentioned that besides the challenge of maximizing the electrical output of a SA, complications such as mismatch [31,32] and partial shading [33] should be treated as well. Recently, different array reconfiguration algorithms were proposed to treat these problems [33–39].

Despite the usage of an advanced technology and scientific attractiveness, most of the evaluated MPPT methods employed either artificial or short-time experimental environmental data. Utilizing long-term experimental data and taking into account the efficiency of the power converter, the MPPT superiority is not obvious [40,41]. The relatively simple and low cost MPPM system may even outperform MPPT-based generation when all the above mentioned factors are taken into account. Moreover, since manufacturing mismatches of modern manufacturers became negligible [31], array reconfiguration is seldom necessary if the illumination is mostly uniform.

The manuscript goal is to present a method of designing an optimally arranged MPPM system and compare its output with MPPT-based solar generation, both exposed to a long term experimental meteorological data of Southern Israel while feeding three common types of loads. The rest of the manuscript is arranged as follows. Section 2 contains the approach to design and modeling of an optimally arranged MPPM system. Section 3 describes the method used for comparison between the two mentioned systems. Results and discussion are given in Section 4 and the manuscript is concluded in Section 5.

2. MPPM system design

Consider a properly sized solar array, consisting of N solar cells or panels, delivering power to a general linear load, shown in Fig. 1 and described by the following I–V characteristic,

$$u_L = u_O + i_L r_O \tag{1}$$

Note that the load, given by (1) may define a pure resistive load ($u_O=0$, $r_O \neq 0$), battery/DC motor load ($u_O \neq 0$, $r_O \neq 0$) or pure voltage source ($u_O \neq 0$, $r_O=0$), representing e.g. a regulated DC bus of a power converter.

A typical I–V curve of a solar cell/panel operating at given temperature and solar irradiation is shown in Fig. 2. It is characterized by the open circuit voltage u_{OC}, short circuit current i_{SC} and maximum power voltage–current pair (u_M, i_M), corresponding to the cell/panel maximum power $p_M = u_M i_M$. In case the solar array consists of m strings of n serially connected cells/panels, its I–V curve is characterized by (neglecting modules mismatch) the open circuit voltage nu_{OC}, short circuit current mi_{SC} and maximum power voltage–current pair (nu_M, mi_M). The goal of MPPM is to ensure that the SA–load operating point for nominal environmental conditions is as close as possible to the SA maximum power point $p_{M,SA} = nmu_M i_M$ by choosing appropriate n and m.

In order to create an optimum array configuration for a given load, the I–V curve is first divided into two parts, using piecewise linear approximation [42], as shown in Fig. 2. The first linear segment starts from the short-circuit point (0, i_{SC}), the second from the open-circuit point (u_{OC}, 0) and both meet at the maximum power point (u_M, i_M). Note that the approximated curve coincides with the original curve in the three characterizing points, therefore employing the approximated model for load matching yields the same results while reducing drastically the computational burden.

The approximated I–V curve of the solar panel may then be expressed as

$$u_{PV} = \begin{cases} u_{OC} - r_1 i_{PV}, 0 \le i_{PV} \le i_M \\ u_M(1+k_I) - r_2 i_{PV}, i_M \le i_{PV} \le i_{SC} \end{cases}, \tag{2}$$

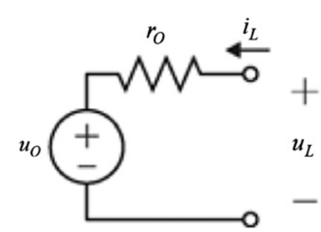


Fig. 1. A general linear load.

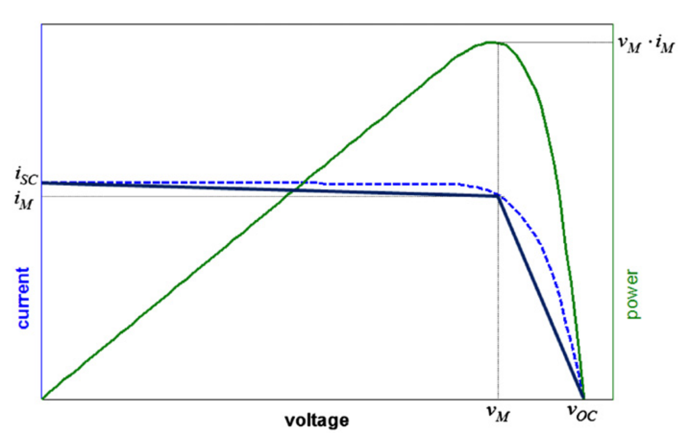


Fig. 2. A general solar panel I–V curve: dashed – exact, solid – linearly approximated.

where

$$r_1 = \frac{u_{OC}-u_M}{i_M},\ r_2 = \frac{u_M}{i_{SC}-i_M},\ k_I = \frac{i_{SC}}{i_{SC}-i_M}. \tag{3}$$

On the $n \times m$ array level, (2) and (3) holds if one substitutes

$$u_{OC,SA} = nu_{OC},\ u_{M,SA} = nu_M,\ i_{SC,SA} = mi_{SC},$$
$$i_{M,SA} = mi_M,\ r_{1,SA} = \frac{n}{m}r_1,\ r_{2,SA} = \frac{n}{m}r_2,\ k_{I,SA} = k_I. \tag{4}$$

Hence the design goal may be formulated by combining (1) and (4) as

$$u_{M,SA} = u_O + i_{M,SA} r_O \tag{5}$$

or

$$nu_M = u_O + mi_M r_O \tag{6}$$

Substituting $N = n \times m$ into (6), the optimal number of serially connected cells is obtained from solving

$$n^2 - n\frac{u_O}{u_M} - \frac{i_M}{u_M} r_O N = 0 \tag{7}$$

as

$$n_{OPT} = 0.5\frac{u_O}{u_M} + \sqrt{0.25\left(\frac{u_O}{u_M}\right)^2 + \frac{i_M}{u_M} r_O N} \tag{8}$$

The optimal number of parallel strings is then given by

$$m_{OPT} = \frac{N}{n_{OPT}} \tag{9}$$

In order for an exact solution to exist, n_{OPT} and m_{OPT} must be integers. Otherwise only an approximate solution exists, i.e. system's operating point does not coincide with the SA maximum power point. Define the matching efficiency as the ratio of operating point power to SA maximum power,

$$\eta_M = \frac{P_L}{P_{M,SA}} \tag{10}$$

If n_{OPT} and m_{OPT} are integers, $\eta_{MPPM} = 1$, otherwise non-optimal n and m are chosen and $\eta_{MPPM} < 1$. Moreover, choosing n as the closest to n_{OPT} integer leads to the highest possible matching efficiency. Note that in order to accurately determine the operating point and matching efficiency, exact rather than approximated SA I–V curve should be employed after the optimization procedure is completed.

Example 1. Consider designing a SA consisting of A300 mono crystalline SunPower solar cells. The standard test conditions (irradiance of 1000 W m^{-2}, solar spectrum of AM 1.5 and cell temperature of 25 °C) data of an A300 cell is given in Table 1 [43]. The SA is intended to charge a 12 V, 0.1 Ω lead–acid battery. The majority of moderate off the shelf solar panels consist of 36 cells, hence the first design step is trying to match a 36-cell panel to the battery. The only arrangement, allowing obtaining a feasible operation point is $n = 36$, $m = 1$. The operational characteristics of such an arrangement are shown in Fig. 3 and summarized in Table 2. The matching efficiency is 66.7%, i.e. only two-thirds of the array rated power are transferred to the load at nominal environmental conditions.

Table 1
A300 cell standard test conditions data.

Open circuit voltage, u_{OC}	0.665 V
Short circuit current, i_{SC}	5.75 A
Maximum power voltage, u_M	0.56 V
Maximum power current, i_M	5.35 A
Rated power, p_M	2.95 W

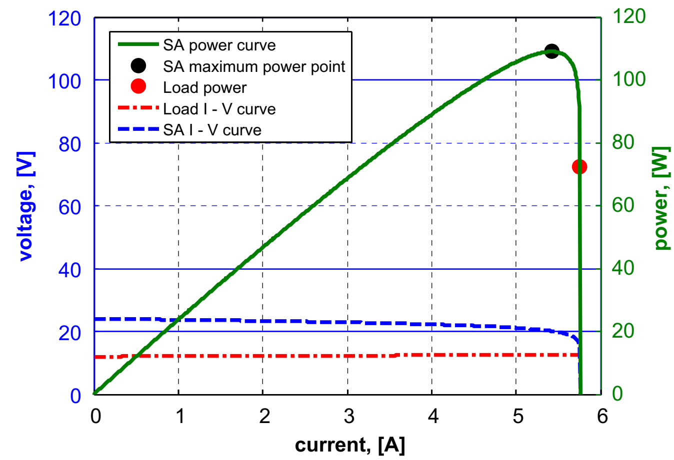


Fig. 3. Operational characteristics of 36 × 1 A300 cell array matched to a 12 V, 0.1 Ω lead–acid battery.

Table 2
Performance summary of a 36 × 1 array matched to a 12 V, 0.1 Ω lead–acid battery.

Load voltage, u_L	12.6 V
Load current, i_L	5.7 A
Load power, p_L	72 W
Maximum SA power, $p_{M,SA}$	108 W
Matching efficiency, η_M	66.7%

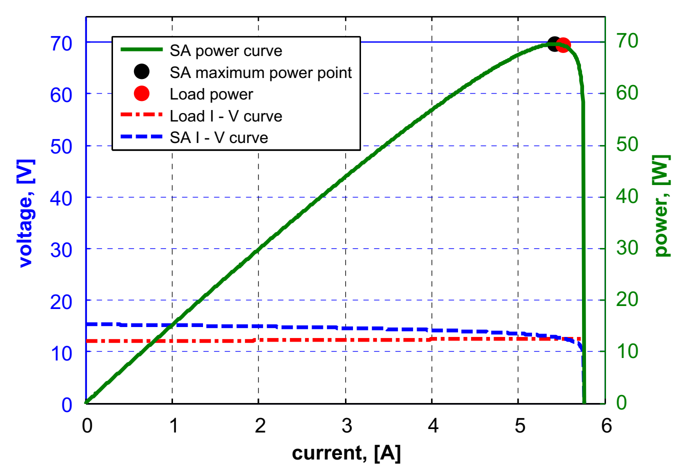


Fig. 4. Operational characteristics of 23 × 1 A300 cell array matched to a 12 V, 0.1 Ω lead–acid battery.

However, substituting solar cell and battery data along with $N = 36$ into (8), results in $n_{OPT} = 22.9$, indicating that 23 series connected cells string will result in the best possible matching. The operational characteristics of 23 × 1 arrangement are shown in Fig. 4 and summarized in Table 3. The matching efficiency at nominal environmental conditions is 99.5%, i.e. virtually all the array rated power is transferred to the load. This means that in order to optimally match a SA array consisting of A300 cells to the particular battery, it should be made up of parallel strings of 23 cells each.

Example 2. Consider designing a SA, feeding the DC bus of a three phase inverter, connected to a 400V grid. Such converters usually operate from DC voltage of 700 V–800 V since they possess buck topology. The SA is to be constructed from SunPower solar panels, consisting of 96 serially connected A300 cells. The array is expected to operate under the nominal operating cell conditions (NOCT), i.e.

under following average environmental conditions: irradiance of 800 W m^{-2}, solar spectrum of AM 1.5 and ambient temperature of 20 °C. The NOCT data of a SunPower panel is given in Table 4 [43].

The rated SA power output is planned to be around 22 kW, hence 100 panels should be purchased at the first glance. The100-panel arrangement, resulting in the most optimal (in terms of power output) 800 V operating point is $n=20$ and $m=5$. The operational characteristics of such an arrangement are shown in Fig. 5 and summarized in Table 5. The matching efficiency is 85.5%, i.e. the actual output of the SA will be 15% short of rated power and an extra string should be added, ending up with 120 panels, delivering 22,560 W of power at average environmental conditions.

Substituting the data into (8) indicates that 16 rather than 20 series connected panels strings will result in the best possible matching. The operational characteristics of 16 × 6 arrangement are shown in Fig. 6 and summarized in Table 6. The matching efficiency at nominal environmental conditions is 99.2%, resulting in the nominal SA power output of 20,950 W, which is 11.4% higher than the 20 × 5 arrangement! Adding an extra string results in a16 × 7 arranged 112 panel array delivering 24,441 W of power at average environmental conditions.

3. MPPM versus MPPT at real long-term weather conditions

The process of a SA–load MPPM is performed for specific site average temperature and irradiance level; however these environmental variables seldom remain constant. Therefore the SA *I–V* curve

Table 3
Performance summary of a 23 × 1 array matched to a 12 V, 0.1 Ω lead–acid battery.

Load voltage, u_L	12.6 V
Load current, i_L	5.45 A
Load power, p_L	68.7 W
Maximum SA power, $p_{M,SA}$	69 W
Matching efficiency, η_M	99.5%

Table 4
SunPower panel NOCT data.

Open circuit voltage, u_{OC}	59.9 V
Short circuit current, i_{SC}	4.75 A
Maximum power voltage, u_M	50.1 V
Maximum power current, i_M	4.4 A
Rated power, p_M	220 W

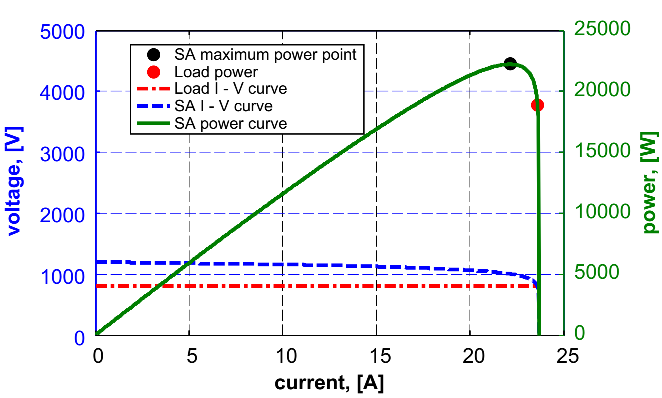


Fig. 5. Operational characteristics of 20 × 5 SunPower panel array matched to an 800 V DC bus.

Table 5
Performance summary of a 20 × 5 SunPower panel array matched to an 800 V DC bus.

Load voltage, u_L	800 V
Load current, i_L	23.5 A
Load power, p_L	18,800 W
Maximum SA power, $p_{M,SA}$	22,000 W
Matching efficiency, η_M	85.5%

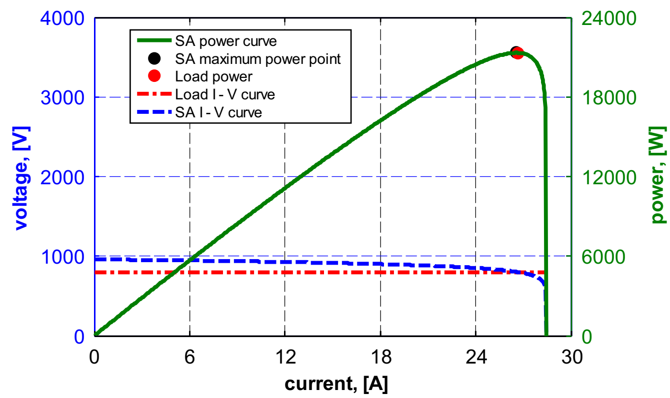


Fig. 6. Operational characteristics of 16 × 6 SunPower panel array matched to an 800 V DC bus.

Table 6
Performance summary of a16 × 6 SunPower panel array matched to an 800 V DC bus.

Load voltage, u_L	800 V
Load current, i_L	26.2A
Load power, p_L	20,950 W
Maximum SA power, $p_{M,SA}$	21,120 W
Matching efficiency, η_M	99.2%

variations, caused by environmental condition changes must be reflected in the evaluation process. In order to accomplish this, a method for deriving arbitrary *I–V* curves of a solar cell/panel for arbitrary temperatures and irradiance levels from the manufacturer provided or experimentally measured standard conditions data, proposed in [44], was adopted. The approach may be related to the class of algorithms, employing numerical methods rather than fitting of any kind to complete the task. The parameters are obtained from a system of normalized nonlinear equations, created by Kirchhoff laws application to the solar cell/panel single-diode equivalent circuit. Several realistic assumptions are made in order to simplify the problem by reducing the number of unknowns. The proposed algorithm was successfully tested on several commercial solar cells, each of different technology.

Ten-year measured meteorological data of the Negev region of Southern Israel was considered [45].Weighted temperature and solar irradiance average values for maximum power production were used as nominal operating conditions for MPPM optimization process. Three different loads, connected to three optimally designed A300-based solar arrays, were tested to demonstrate the outcomes of the discussed method. The first load was represented by a near-ideal voltage source with $u_O=12$ V and negligible resistance of $r_O=0.01$ Ω. For this load, the optimization procedure resulted in 27 × 1 cell arrangement. The second one was modeled by a voltage source $u_O=8$ V with internal resistance of $r_O=1.5$ Ω. The optimization procedure indicated that 26 × 1 strings would

maximize the power output for nominal environmental conditions. A pure resistor $r_O=4.7\ \Omega$ was employed as the third load with 25×1 optimal cell arrangement.

Two solar systems, based on the same optimally arranged SA were considered for each load: one consisting of a SA connected directly to the load without any intermediate electronic devices; the other including a lossless MPPT-operated DC-DC converter. The lossless MPPT system was assumed to extract the maximum possible amount of energy from the sun and passing into the load at any given moment. The efficiency of modern practical MPPT converters was then employed for ideal performance correction.

4. Results and discussion

Performances of both systems were estimated by dedicated MATLAB-based routine for each above mentioned load. Ten-year averaged monthly amount of energy produced by each system and percentage difference between the directly connected and the idealized MPPT-operated solar system outputs were calculated.

The results were as follows. Systems feeding the first type of load (nearly ideal voltage source) possess the smallest difference between the outputs of both systems, as shown in Fig. 7. The percentage difference varies between 0.5% and 3% with an annual average of $\Delta W=1.08\%$.

When the load was represented by a voltage source with a fairly substantial internal resistance, the energy difference varied in a 3%–17% range with a mean annual value of $\Delta W=6.1\%$, as shown in Fig. 8.

Pure resistive load causes the highest annual average deviation of the directly connected solar system output energy from a possible maximum value (see Fig. 9). In this case the energy difference fluctuates in the range of 15% - 50% with an annual mean of $\Delta W=23\%$.

In order to attain a deeper understanding of the obtained results, recall a well-known behavior of solar panels under varying environmental conditions. Fig. 10 presents the power curves of A300 cell for different temperatures and irradiance level. Consider the left subplot of Fig. 10 first, where the A300 power curves are shown for 25 °C cell temperature and 0.2 Sun–

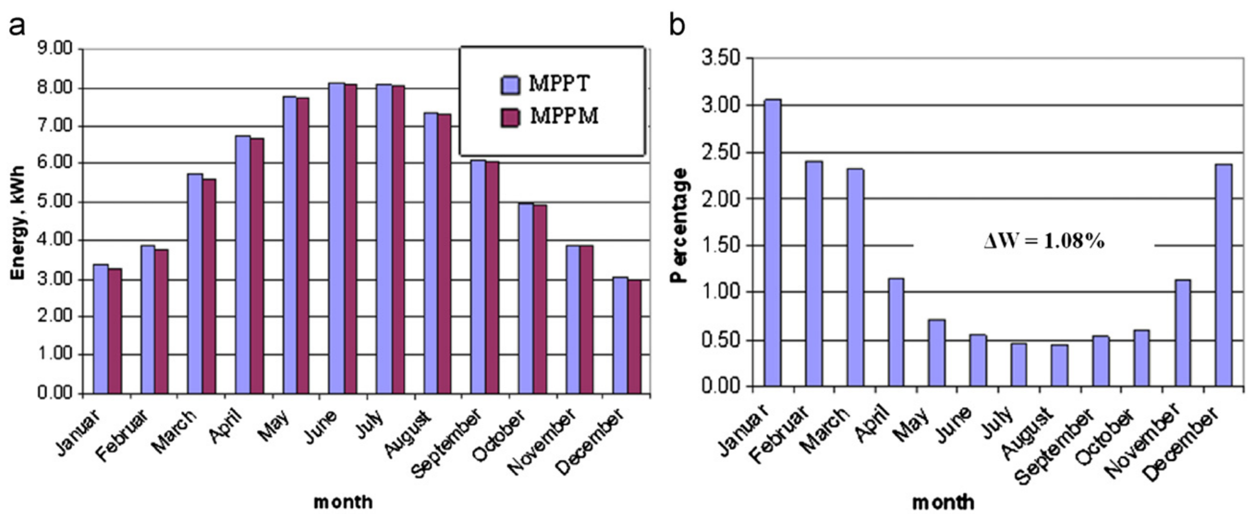


Fig. 7. Test results for $n=27$, $m=1$, $r_O=0.01\ \Omega$, $u_O=12$ V; (a) Energy production: MPPT-based versus MPPM-based and (b) percentage difference between energy productions.

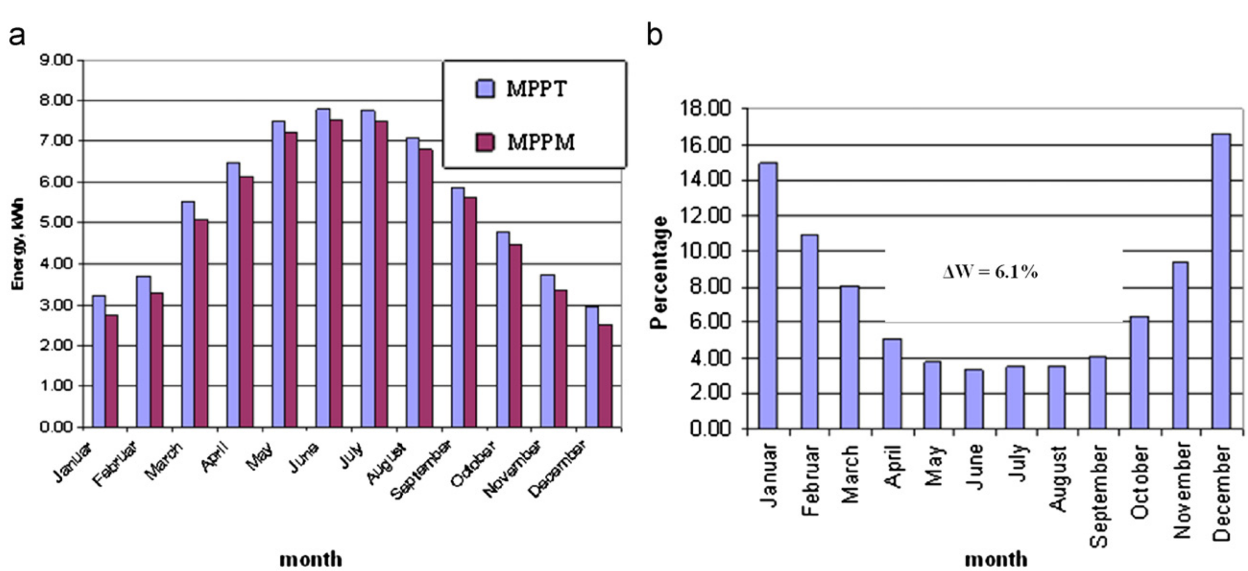


Fig. 8. Test results for $n=26$, $m=1$, $r_O=1.5\ \Omega$, $u_O=8$ V; (a) Energy production: MPPT-based versus MPPM-based and (b) percentage difference between energy productions.

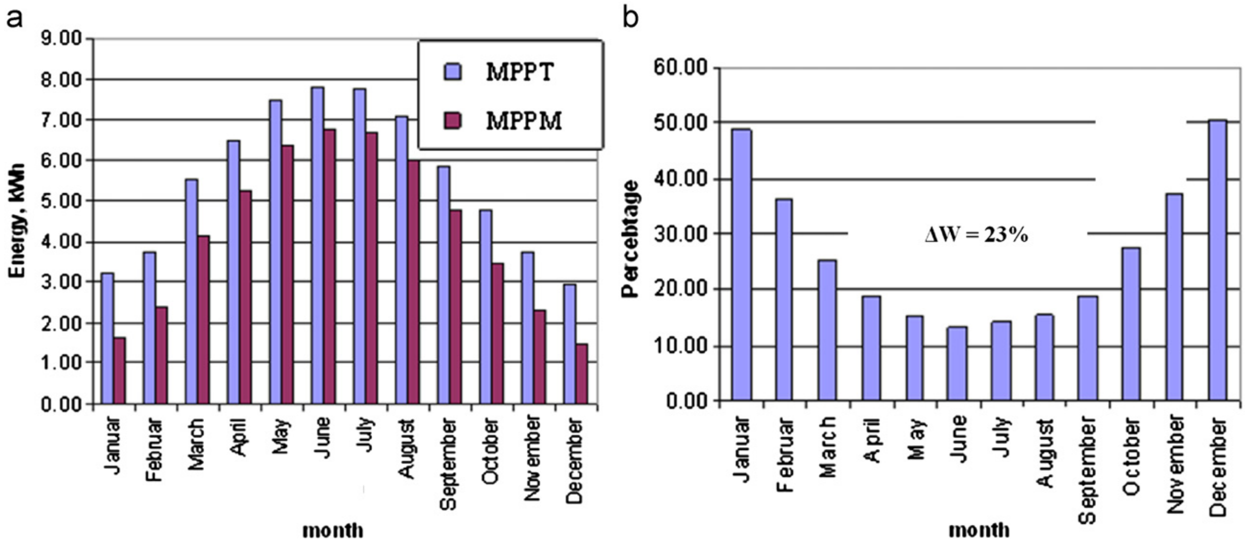


Fig. 9. Test results for n=25, m=1, r_O=4.7 Ω, u_O=0 V; (a) Energy production: MPPT-based versus MPPM-based and (b) percentage difference between energy productions.

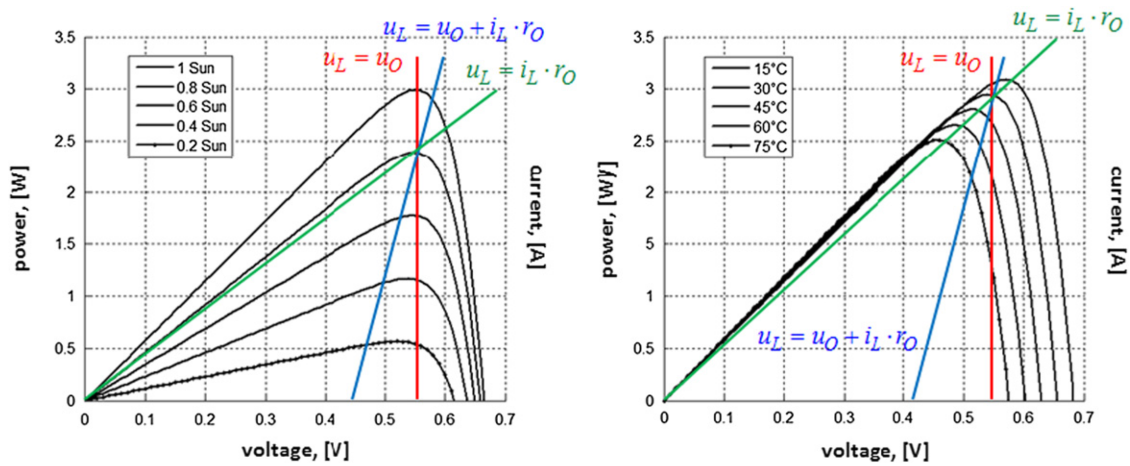


Fig. 10. A300 cell power curve dependence on varying environmental conditions. Left – temperature of 25 °C and different irradiance levels and right – irradiance of 1 Sun and different temperatures. (For interpretation of the references to color in this figure legend, the reader is referred to the web version of this article.)

1 Sun different irradiance levels. Suppose that the average irradiance level at some site is 0.8 Sun, hence correct matching should create an operating point at the SA power point, corresponding to 0.8 Sun MPP. Note that the MPP's of the entire irradiance power curves possess nearly the same u_M, hence a pure voltage source load (red line), matched to a particular MPP, resides in a close proximity to all the other MPPs and is superficial to irradiance level variations. A load, represented by a voltage source with a substantial internal resistance (blue line) is much more sensitive to the irradiance variations, though stable operating points exist not far away from the MPP for each irradiance level. This is not the case when a pure resistive load (green line) is employed. When the irradiance level increases from the nominal one, an operating point exists far from the MPP. However, when the irradiance level decreases, the power production is sharply reduced.

As to right subplot of Fig. 10, where the A300 power curves are shown for 1 Sun irradiance level and cell temperatures, the situation is opposite. The resistive load possesses the best match to varying temperatures, while the constant voltage load is expected to yield the poorest performance, though stable operating points exist for the entire temperature range. However, the irradiance variations are usually much more severe and stochastic that the temperature variations. Moreover, in hot countries such as Israel, once a cell/panel heats up, its temperature remains relatively unchanged throughout a day, since its thermal inertia is relatively high and the ambient temperature is stable. Therefore the load, best suited to the irradiance variations, is expected to yield the highest performance, and this is demonstrated by this work.

The results indicate that the deviation of the energy produced by a directly connected system from the maximum possible value strongly depends on the load type. In addition, meteorological data also plays an important role in annual energy production. The temperature in Israel is relatively stable during the day and the amount of slow-moving clouds (causing significant irradiance and temperature variations) is low. It is also clear, that in case of linear, time invariant loads, the usage of MPPT-based conversion is justified only if the energy deviation is more than the typical losses in MPPT-operated converter (6–10% [40,41,46]), i.e. in the case of pure resistive load only.

5. Conclusion

An approach to optimal arrangement of a solar array for glueless matching to a known linear load was discussed in the

paper. Array performance was investigated for different loads under real weather conditions. It was shown that the deviation of the energy produced by a converterless system from the maximum possible value strongly depends on both load and meteorological data. Test results indicated that only in case of a pure resistive load the MPPT-based solar system usage is justified. In case of a load represented by a voltage source with internal resistance, losses in a real MPPT-operated converter are on the par or higher than the converterless system produced energy deviation from the maximum possible value.

References

[1] Lenzen M. Current state of development of electricity-generating technologies: a literature review. Energies 2010;3:462–591.
[2] Raugei M, Frankl P. Life cycle impacts and costs of photovoltaic systems: current state of the art and future outlooks. Energy 2009;34:392–9.
[3] Parida B, Iniyan S, Goic R. A review of solar photovoltaic technologies. Renewable & Sustainable Energy Reviews 2011;15:1625–36.
[4] Razykov T, Ferekides C, Morel D, Stefanakos E, Ullal H, Upadhyaya H. Solar photovoltaic electricity: current status and future prospects. Solar Energy 2011;85:1580–608.
[5] Lee CY, Chou PC, Chiang CM, Lin CF. Sun tracking systems: a review. Sensors 2009;9:3875–90.
[6] Mousazadeh H, Keyhani A, Javadi A, Mobli H, Abrinia K, Sharifi A. A review of principles and sun-tracking methods for maximizing solar systems output. Renewable & Sustainable Energy Reviews 2009;13:1800–18.
[7] Enslin J. Maximum power point tracking: a cost saving necessity in solar energy systems. Renewable Energy 1992;2:543–9.
[8] Cabral C, Filho D, Diniz A, Martins J, Toledo O, Neto L. A stochastic method for stand-alone photovoltaic system sizing. Solar Energy 2010;84:1628–36.
[9] Salameh Z, Borowy B, Amin A. Photovoltaic module-site matching based on the capacity factors. IEEE Transactions on Energy Conversion 1995;10:326–32.
[10] Khouzam K. The load matching approach to sizing photovoltaic systems with short-term energy storage. Solar Energy 1994;53:403–9.
[11] Badescu V. Simple optimization procedure for silicon based solar cell interconnection in a series-parallel PV module. Energy Conversion and Management 2006;47:1146–58.
[12] Singer S, Braunstein A. Optimum operation of a combined system of a solar cell array and a DC motor. IEEE Transactions on Power Apparatus and Systems 1981;100:1193–7.
[13] Applebaum J. The quality of load matching in a direct-coupling photovoltaic system. IEEE Transactions on Energy Conversion 1987;2:534–41.
[14] Khouzam K. Optimum load matching in direct-coupled photovoltaic power systems – application to resistive loads. IEEE Transactions on Energy Conversion 1990;5:265–71.
[15] Khouzam K, Khouzam L, Groumpos P. Optimum matching of ohmic loads to the photovoltaic array. Solar Energy 1991;46:101–8.
[16] Khouzam K, Khouzam L. Optimum matching of direct-coupled electromechanical loads to a photovoltaic generator. IEEE Transactions on Energy Conversion 1993;8:343–9.
[17] Ibrahim O. Load matching to photovoltaic generators. Renewable Energy 1995;6:29–34.
[18] Hohm D, Ropp M. Comparative study of maximum power point tracking algorithms. Progress in Photovoltaics: Research and Applications 2003;11:47–62.
[19] Salas V, Olias E, Barrado A, Lazaro A. Review of the maximum power point tracking algorithms for stand-alone photovoltaic systems. Solar Energy Materials & Solar Cells 2006;90:1555–78.
[20] Jain S, Agarwal V. Comparison of the performance of maximum power point tracking schemes applied to single-stage grid-connected photovoltaic systems. IET Electric Power Applications 2007;1:753–62.
[21] Esram T, Chapman P. Comparison of photovoltaic array maximum power point tracking techniques. IEEE Transactions on Energy Conversion 2007;22:439–49.
[22] Faranda R, Leva S. Energy comparison of MPPT techniques for PV systems. WSEAS Transactions on Power Systems 2008;6:446–55.
[23] Azevedo G, Cavalcanti M, Oliveira K, Neves F, Lin Z. Comparative evaluation of maximum power point tracking methods for photovoltaic systems. Journal of Solar Energy Engineering 2009;131:61–8.
[24] Snyman D, Enslin J. An experimental evaluation of MPPT converter topologies for PV installations. Renewable Energy 1993;3:841–8.
[25] Walker G, Sernia P. Cascaded DC–DC converter connection of photovoltaic modules. IEEE Transactions on Power Electronics 2004;19:1130–9.
[26] Blaabjerg F, Chen Z, Kjaer S. Power electronics as efficient interface in dispersed power generation systems. IEEE Transactions on Power Electronics 2004;19:1184–94.
[27] Kjaer S, Pedersen J, Blaabjerg F. A review of single-phase grid-connected inverters for photovoltaic modules. IEEE Transactions on Industry Applications 2005;41:1292–306.
[28] Enrique J, Duran E, Sidrach-de-Cardona M, Andujar J. Theoretical assessment of the maximum power point tracking efficiency of photovoltaic facilities with different converter topologies. Solar Energy 2007;81:31–8.
[29] Li Q, Wolfs P. A review of the single phase photovoltaic module integrated converter topologies with three different DC link configurations. IEEE Transactions on Power Electronics 2008;23:1320–33.
[30] de Brito M, Junior L, Sampaio L, Melo G, Canesin C. Evaluation of the main MPPT techniques for photovoltaic applications. IEEE Transactions on Industry Applications 2013;60:1156–67.
[31] Spertino F, Akilimali J. Are manufacturing *I–V* mismatch and reverse currents key factors in large photovoltaic arrays? IEEE Transactions on Industrial Electronics 2009;56:4520–31.
[32] Petrone G, Ramos-Paja C. Modeling of photovoltaic fields in mismatched conditions for energy yield evaluations. Electric Power Systems Research 2011;81:1003–13.
[33] Villa L, Picault D, Raison B, Bacha S, Labonne A. Maximizing the power output of partially shaded photovoltaic plants through optimization of the interconnections among its modules. IEEE Journal of Photovoltaics 2012;2:154–63.
[34] Zerhouni F, Zegrar M, Benmessaoud M, Stambouli A, Midoun A. Optimum load matching by an array reconfiguration in photovoltaic generators. Energy and Fuels 2012;24:6126–30.
[35] Nguyen D, Lehman B. An adaptive solar photovoltaic array using model-based reconfiguration algorithm. IEEE Transactions on Industrial Electronics 2008;55:2644–54.
[36] Velasco-Quesada G, Guinjoan-Gispert F, Pique-Lopez R, Roman-Lumbreras M, Conesa-Roca M. Electrical PV array reconfiguration strategy for energy extraction improvement in grid-connected PV systems. IEEE Transactions on Industrial Electronics 2009;56:4319–31.
[37] Obane H, Okajima K, Oozeki T, Ishii T. PV System with reconnection to improve output under nonuniform illumination. IEEE Journal of Photovoltaics 2012;2:341–7.
[38] El-Dein M., Kazerani M, Salama M. An optimal total cross tied interconnection for reducing mismatch losses in photovoltaic arrays. IEEE Transactions on Sustainable Energy, http://dx.doi.org/10.1109/TSTE.2012.2202325, in press.
[39] El-Dein M, Kazerani M, Salama M. Optimal photovoltaic array reconfiguration to reduce partial shading losses. IEEE Transactions on Sustainable Energy, http://dx.doi.org/10.1109/TSTE.2012.2208128, in press.
[40] Li S, Haskew T, Li D, Hu F. Integrating photovoltaic and power converter characteristics for energy extraction study of solar PV systems. Renewable Energy 2011;36:3238–45.
[41] Demoulias C. A new simple analytical method for calculating the optimum inverter size in grid-connected PV plants. Electric Power Systems Research 2010;80:1197–204.
[42] Averbukh M. One aspect of optimal construction of solar panels. In: Proceedings of the 13th Sede Boqer Symposium on Solar Electricity Production, Israel; 2005. p. 149–52.
[43] ⟨www.sunpowercorp.com⟩; 2012 [accessed 18.09.12].
[44] Averbukh M, Lineykin S, Kuperman A. Obtaining small photovoltaic array operational curves for arbitrary cell temperatures and solar irradiation densities from standard conditions data. Progress in Photovoltaics: Research and Applications, http://dx.doi.org/10.1002/pip.2199, in press.
[45] Averbukh M, Kuperman A. Real weather conditions impact on optimally arranged solar cell array. In: Proceedings of the 14th Sede Boqer Symposium on Solar Electricity Production, Israel; 2007. p. 107–10.
[46] ⟨www.linuouk.com⟩; 2012 [accessed 18.09.12].